nature biotechnology

Specification of transplantable astroglial subtypes from human pluripotent stem cells

Robert Krencik[1,2], Jason P Weick[2,6], Yan Liu[3,6], Zhi-Jian Zhang[2] & Su-Chun Zhang[1–5]

Human pluripotent stem cells (hPSCs) have been differentiated efficiently to neuronal cell types. However, directed differentiation of hPSCs to astrocytes and astroglial subtypes remains elusive. In this study, hPSCs were directed to nearly uniform populations of immature astrocytes (>90% S100β$^+$ and GFAP$^+$) in large quantities. The immature human astrocytes exhibit similar gene expression patterns as primary astrocytes, display functional properties such as glutamate uptake and promotion of synaptogenesis, and become mature astrocytes by forming connections with blood vessels after transplantation into the mouse brain. Furthermore, hPSC-derived neuroepithelia, patterned to rostral-caudal and dorsal-ventral identities with the same morphogens used for neuronal subtype specification, generate immature astrocytes that express distinct homeodomain transcription factors and display phenotypic differences of different astroglial subtypes. These human astroglial progenitors and immature astrocytes will be useful for studying astrocytes in brain development and function, understanding the roles of astrocytes in disease processes and developing novel treatments for neurological disorders.

Astroglial cells are the most abundant cell type in the human brain and spinal cord and are now understood to be as important as neurons for brain function[1,2]. During development, astroglial progenitors are specified after neurogenesis, although their identity is not well defined owing to lack of reliable markers[3,4]. Astroglial progenitors differentiate to immature astrocytes, which are essential for the formation of functional synapses[5,6]. In the adult brain, mature astrocytes insulate synapses and remove excess transmitters, such as glutamate, released during neural excitation, thus preventing excitotoxicity[7]. Astrocytes are crucial for maintaining a homeostatic environment for the healthy brain by supporting neurovascular coupling at the blood-brain barrier, regulating blood flow[8] and supplying energy metabolites throughout the brain[9]. Abnormalities in astroglial cells are implicated in a number of human pathologies, including astrocytomas, epilepsy[10], Alexander disease[11] and neurodegenerative diseases[12,13]. Thus, understanding how to regulate the generation, maintenance and functions of human astroglial cells will likely benefit the treatment of a range of neurological injuries and diseases.

Astrocytes are heterogeneous in many respects, including morphology, growth rates[14], gene expression profiles[15,16], electrophysiological properties[17], gap junction coupling and calcium wave propagation dynamics[18,19]. However, how these various astroglial phenotypes are gained is largely unknown. In the mouse and chick spinal cord, homeodomain and helix-loop-helix (HLH) transcription factors are expressed in progenitors of specific dorsal-ventral domains, and genetic alterations of these factors shift the gene expression pattern of astrocytes generated from these domains[20–22]. This suggests that astroglial diversity may be determined through regional patterning (specification of regional identities) of progenitor cells. However, it remains unknown whether astroglial subtypes may be generated by simply patterning neural stem or progenitor cells, especially human stem cells.

In the present study, we describe a chemically defined differentiation system for efficient generation of immature astrocytes from hPSCs, including embryonic (hESCs) and induced pluripotent stem cells (iPSCs). HPSCs were first differentiated to neuroepithelial cells and specified to regional progenitors. They were then expanded as free-floating clusters or 'astrospheres' in the presence of growth factors, with periodic dissociation into single cells to promote gliogenesis. Astroglial differentiation from human neural stem cells or fetal tissues often requires serum, and the capacity to expand is limited. In contrast, the present technology allows generation of a nearly pure population of astroglial progenitors in a chemically defined system, which can be expanded to large quantities. Furthermore, the resultant cell population is free of immune cells such as microglia, and regionally and functionally specialized astroglial subtypes can be readily generated. We apply this approach to three different hPSC lines and show that it yields progenitors that can expand in culture for a long time, producing an estimated 2.8×10^{12} immature astrocytes at 6 months from one hPSC cell. Notably, we find that regionally and functionally distinct human astroglial subtypes are induced by patterning neuroepithelial cells at an early stage, and that they maintain their identities after transplantation into ectopic mouse brain regions, providing a possible cellular source for regenerative medicine.

RESULTS

Differentiation to astroglia follows developmental principles

Astroglial cells appear after neurons during vertebrate development. We hypothesized that hPSC-derived neural progenitors, after

[1]Neuroscience Training Program, University of Wisconsin-Madison, Madison, Wisconsin, USA. [2]Waisman Center, University of Wisconsin–Madison, Madison, Wisconsin, USA. [3]Department of Human Anatomy and Histology, Fudan University Shanghai Medical School, Shanghai, China. [4]Department of Neuroscience, University of Wisconsin–Madison, Madison, Wisconsin, USA. [5]Department of Neurology, School of Medicine and Public Health, University of Wisconsin–Madison, Madison, Wisconsin, USA. [6]These authors contributed equally to this work. Correspondence should be addressed to S.-C.Z. (zhang@waisman.wisc.edu).

Received 10 January; accepted 20 April; published online 22 May 2011; doi:10.1038/nbt.1877

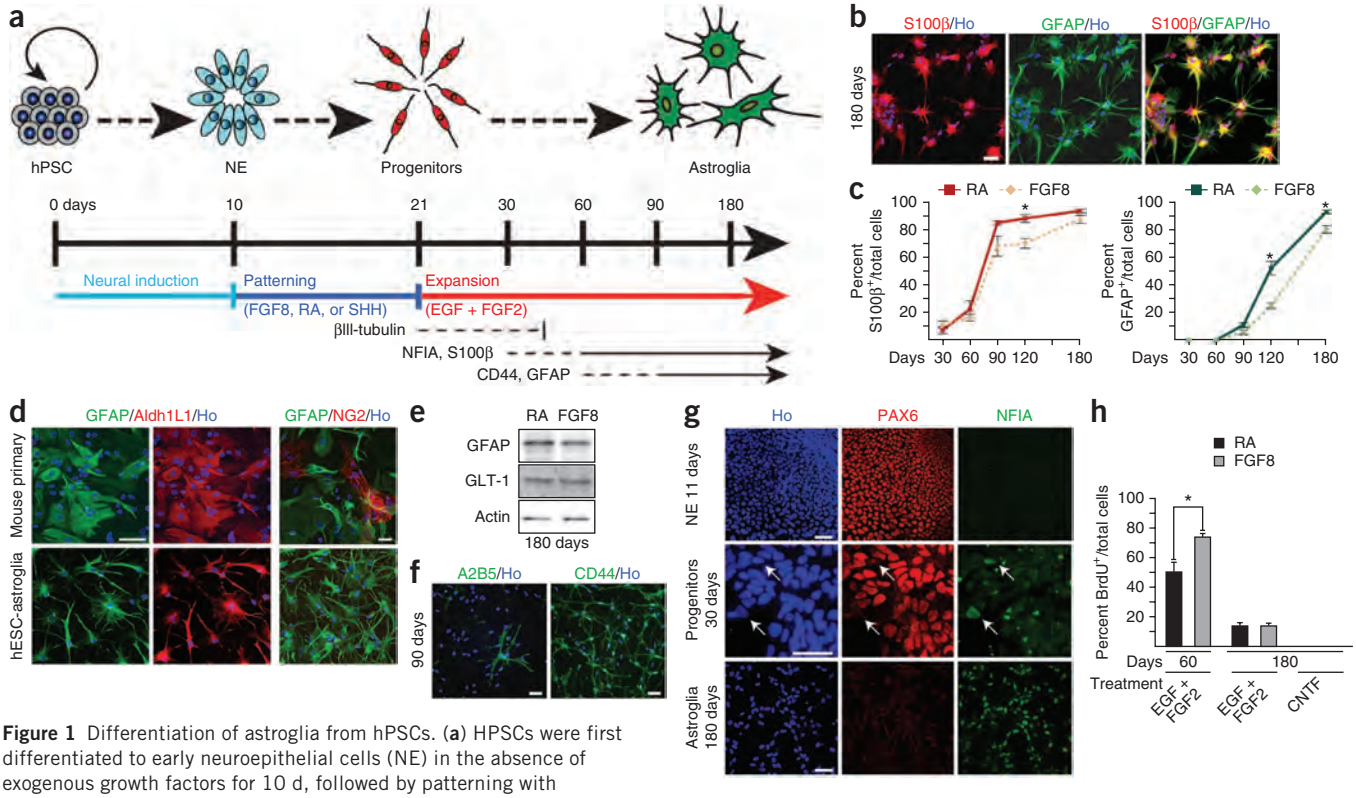

Figure 1 Differentiation of astroglia from hPSCs. (**a**) HPSCs were first differentiated to early neuroepithelial cells (NE) in the absence of exogenous growth factors for 10 d, followed by patterning with morphogens between days 10 and 21. The neural/astroglial progenitors were expanded in the presence of EGF and FGF2, during which progenitors were differentiated for 7 d with CNTF every 30 d for characterization with cell type–specific markers. RA, retinoic acid. (**b**) At day 180, immature astrocytes display a stellate morphology, express S100β in both the cytoplasm and nuclei, and express GFAP in a filamentous pattern throughout the cytoplasm. Nuclei are indicated by Hoechst (Ho) staining. (**c**) Temporal course comparison of S100β (120 d, $P = 0.0055$) and GFAP (120 d, $P = 0.001$; 180 d, $P = 0.0066$) expression of retinoic acid– and FGF8-specified astroglia (from three separate passages of the H9 hESC line) among total cells. (**d**) hESC-astroglia cells express Aldh1L1, but not NG2, in contrast to mouse primary astrocytes. (**e**) Western blotting analysis confirms the expression of GFAP and GLT-1 in day 180 astroglia (RA and FGF8, as in **c**). (**f**) Subsets of astroglia express A2B5, whereas the majority of immature astrocytes express CD44 by 90 d. (**g**) NFIA is not expressed in early neuroepithelial cells at day 11, but it begins to be expressed in a small number of progenitors with concomitant down-regulation of PAX6 at day 30 (arrows). By day 180, all cells express NFIA. (**h**) Incorporation of BrdU by retinoic acid– and FGF8-specified astroglial progenitors at 60 d ($n = 6$, $P = 0.0043$) demonstrates differential proliferation of subtypes. By 180 d, BrdU uptake is not different between groups, and is completely absent in cells after removal of growth factors and addition of CNTF. Scale bars, 50 μM. Data are represented as mean ± s.e.m. *, $P < 0.05$.

temporal expansion, become gliogenic and generate astroglia under conditions that facilitate glial differentiation (**Fig. 1a**). HPSCs were directed to neuroepithelial cells, followed by differentiation to neural progenitors from days 10 to 21 in the presence of either the posterior patterning molecule retinoic acid (0.5 μM), or the anterior patterning morphogen fibroblast growth factor 8 (FGF8, 50 ng/ml)[23,24] to examine whether early specification leads to divergent astroglial subtypes (see below). Differentiation of day 30 retinoic acid–treated progenitors from the H9 hESC line showed that a small population of cells (7.7% ± 1.5) were S100β$^+$ and hardly any cells (<0.1%) were GFAP$^+$, the two common astroglial markers. Most other cells were shaped like columnar epithelial cells, indicative of progenitor identity, whereas some exhibited neuronal phenotypes and were positive for the neuron-specific marker βIII-tubulin (4.4% ± 0.8), which decreased over time. At increasing time periods, the number of S100β$^+$ cells continued to increase, and displayed the typical stellate morphology of astroglia (**Fig. 1b**,**c**). Similarly, GFAP-expressing cells began to appear after 8 weeks, and the percentages increased over time (**Fig. 1b**,**c**). The GFAP$^+$ cells always co-labeled with S100β. A similar progression of astroglial marker expression was observed in cells that were specified with FGF8, but considerably slower at certain time points (**Fig. 1c**). Aldh1L1, a recently identified marker for the astroglial lineage[25], but not NG2, a proteoglycan expressed by NG2 cells[26], was also detected in GFAP$^+$ cells (**Fig. 1d**). Western blotting analysis of day 180 immature astrocytes demonstrated the expression of GFAP and the astrocyte-specific glutamate transporter GLT-1 (**Fig. 1e**). These results further confirmed their astroglial identity. Leukemia inhibitory factor (LIF) had a similar effect as ciliary neurotrophic factor (CNTF) in increasing the proportion of GFAP$^+$ cells after treatment of the day 180 progenitors for 6 d (**Supplementary Fig. 1a**).

To identify progenitors during astroglial differentiation, we examined putative glial progenitor markers, including A2B5, CD44 (ref. 27) and NFIA[28]. A2B5 was expressed in a subset of S100β$^+$ cells at days 30 and 90 (9.8% ± 3.2 and 8.7% ± 2.1, respectively), and the percentage decreased as cells became GFAP$^+$. CD44, however, was not observed until day 60, and by day 90, 79.5 ± 1.9% of S100β$^+$ cells expressed CD44 (**Fig. 1f**). NFIA, which was completely absent in PAX6$^+$ neuroepithelial cells at day 11, began to be expressed by day 30 as cells downregulated PAX6. Day 180 astroglial cells all expressed high levels of NFIA (**Fig. 1g**). Thus, astroglial progenitors or immature astrocytes can be identified by expression of NFIA-S100β at 4–8 weeks after hPSC differentiation, and more mature astrocytes can be marked additionally by CD44-GFAP after 8–12 weeks of differentiation. This expression pattern is remarkably similar to that of *in vivo* human development[29,30].

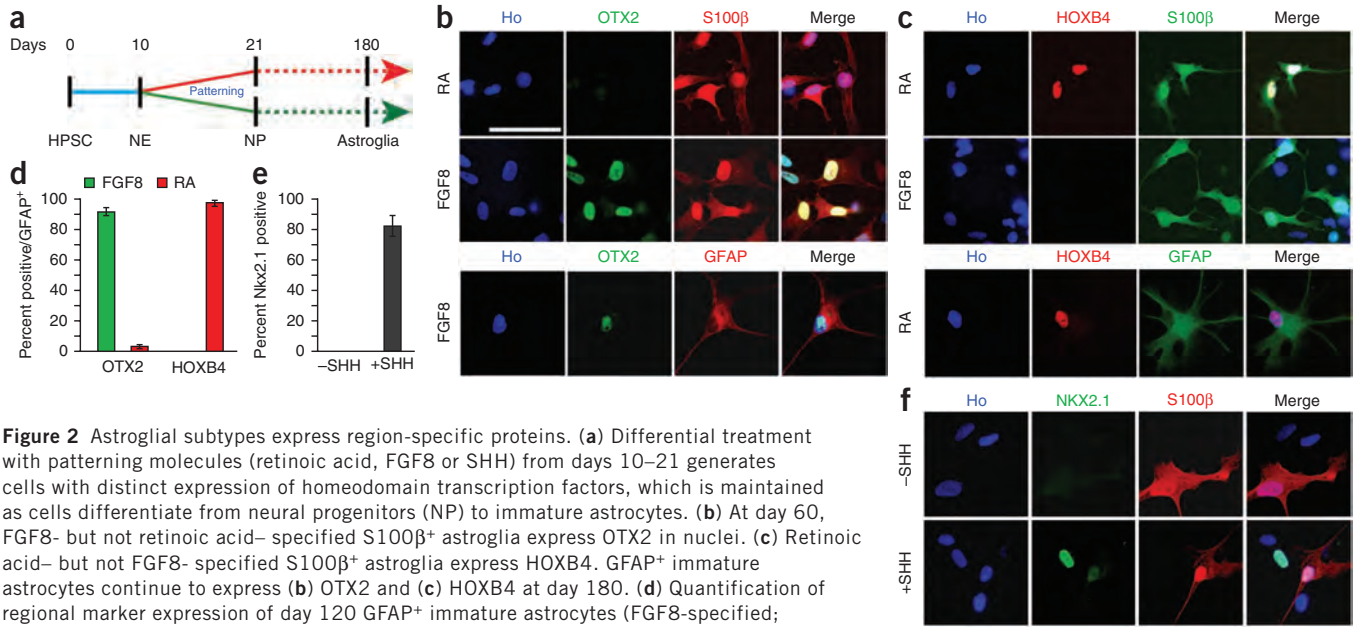

Figure 2 Astroglial subtypes express region-specific proteins. (**a**) Differential treatment with patterning molecules (retinoic acid, FGF8 or SHH) from days 10–21 generates cells with distinct expression of homeodomain transcription factors, which is maintained as cells differentiate from neural progenitors (NP) to immature astrocytes. (**b**) At day 60, FGF8- but not retinoic acid– specified S100β$^+$ astroglia express OTX2 in nuclei. (**c**) Retinoic acid– but not FGF8- specified S100β$^+$ astroglia express HOXB4. GFAP$^+$ immature astrocytes continue to express (**b**) OTX2 and (**c**) HOXB4 at day 180. (**d**) Quantification of regional marker expression of day 120 GFAP$^+$ immature astrocytes (FGF8-specified; OTX2 = 92.1% ± 2.5, HOXB4 = 0. GFAP$^+$ retinoic acid–specified; OTX2 = 3.2% ± 1.3, HOXB4 = 97.6% ± 2.1). (**e**) Quantification of day 30 ventralized astroglial progenitors (-SHH; NKX2.1 = 0. +SHH; NKX2.1 = 82.6% ± 7.0). (**f**) Day 60 S100β$^+$ astroglia differentiated from SHH-ventralized neural progenitors express NKX2.1. Scale bar, 50 μM.

Quantitative reverse transcription (qRT)-PCR analysis indicated that the hPSC-derived day 210 astroglia expressed high levels of additional astroglial genes, including NF1X, CHL1, GLAST, GLT1 and aquaporin 4 (**Supplementary Fig. 1c**). Taken together, these results not only confirmed the astroglial identity but also suggested functional attributes of the hPSC-derived astroglia.

The hPSC-derived astroglial progenitors were expanded continuously for at least 8 months and survived freeze-thaw cycles. BrdU pulse-labeling for 10 h in day-60 progenitors revealed a higher percentage of cells undergoing DNA synthesis, a correlate of cellular proliferation, in FGF8-specified progenitors (74.2% ± 2.0, $n = 6$) compared to retinoic acid–specified progenitors (50.6% ± 6.1) (**Fig. 1h**). At 6 months, the extent of BrdU labeling decreased, the two groups exhibited a similar proliferation rate, and removal of growth factors inhibited DNA synthesis (**Fig. 1h**). In the presence of EGF and FGF2, the retinoic acid–specified astroglial progenitors maximally expanded at a rate of 7.6 ± 1.2 times every 6 d for 4–5 months when seeded at 24,000 cells/cm^2. Although hESCs and iPSCs exhibit slightly different efficiency in neuroepithelial cell generation[31], differentiation of neuroepithelial cells and expansion of astroglial progenitors from these various hPSC lines (H9, H7, (IMR90)-4) were similarly efficient. If one hPSC is differentiated to neuroepithelial cells, converted to glial progenitors and then expanded in suspension, an estimated 2.8×10^{12} immature astrocytes can be generated in 6 months, taking into account any cell loss during the procedure. Therefore, this method allows generation of large quantities of astroglia.

Regionally specified neuroepithelia generate astroglial subtypes

Like neurons, astrocytes in different regions of the central nervous system (CNS) exhibit different phenotypes. We hypothesized that regionally distinct astroglia may be specified from hPSCs in the same way as for neuronal cell types through patterning of neuroepithelial cells and subsequent differentiation (**Fig. 2a**). At day 30 of differentiation from H9 hESCs, nearly all of the cells patterned with retinoic acid during days 10–21 expressed the hindbrain/spinal cord-specific transcription factor HOXB4 (98.6% ± 0.7, $n = 5$) and very few expressed the midforebrain marker OTX2 (3.1% ± 0.8). The FGF8-treated cells, similar to those not treated with FGF8 (ref. 32), expressed OTX2 (95.4% ± 3.0) and none expressed HOXB4. This expression pattern of homeodomain transcription factors persisted as cells began to express astroglial markers S100β and GFAP (**Fig. 2b–d** and **Supplementary Fig. 2a**), but with a slight decrease of OTX2 in GFAP$^+$ astrocytes. A similar expression pattern of homeodomain transcription factors was observed in primary astrocytes isolated from the mouse embryonic brain and spinal cord (**Supplementary Fig. 2c**), and in astrocytes specified from iPSCs (**Supplementary Fig. 3**). qRT-PCR analysis confirmed differential expression of additional homeodomain genes and functional genes in the anterior and posterior immature astrocytes (**Supplementary Fig. 2b**), signaling potential functional diversities.

To determine whether astroglia with a dorsal-ventral distinction can also be specified, neuroepithelial cells were treated with or without the ventralizing factor sonic hedgehog (SHH, 500 ng/ml). In the absence of morphogens, hESC-derived neural progenitors exhibit a dorsal telencephalic phenotype[33]; none of the astroglial progenitors expressed the ventral marker NKX2.1 (**Fig. 2e,f**). In contrast, the majority of astroglial progenitors (day 30) differentiated from the SHH-treated neuroepithelial cells were labeled for NKX2.1, though NKX2.1 was noticeably decreased upon S100β expression (**Fig. 2f**). Regional marker expression was confirmed in subsets of GFAP$^+$ astrocytes in P1 mouse brain and spinal cord sections (**Supplementary Fig. 2d**). Together, our results indicate that region-specific astroglia can be specified from hPSCs in the same way as for region-specific neuronal types. The same trend of astroglial differentiation and regional patterning was observed with the H7 hESC line and the (IMR90)-4 iPSC line (**Supplementary Fig. 3a,b**).

HPSC-derived immature astrocytes are functional

In contrast to neurons, astroglia are described as passive cells because they cannot generate action potentials and their voltage-gated currents decrease during maturation[34]. Whole-cell patch clamp recordings of

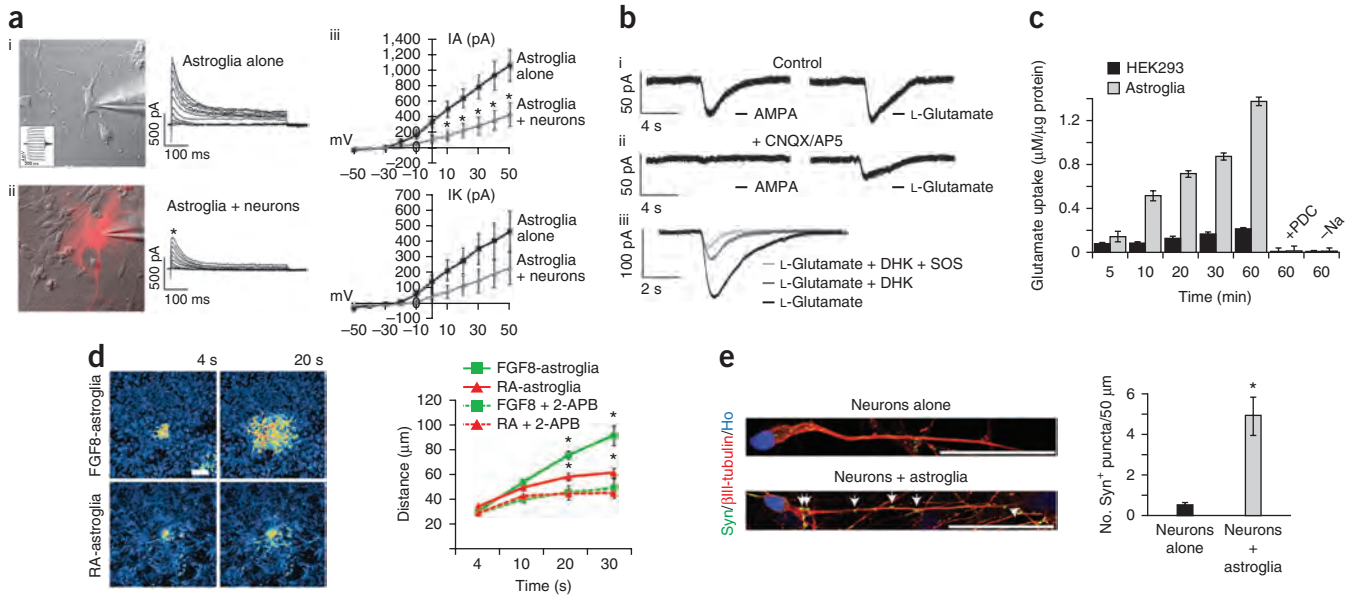

Figure 3 Functional characteristics of hPSC-derived immature astrocytes. (**a**) Immature astrocytes were analyzed by whole-cell patch clamping. (i–iii) Voltage steps (clamped at –70 mV and stepped from –50 to +50 mV at 10 mV increments for 500 ms) induced outward currents in red fluorescent–labeled 4-month astroglia, which significantly decreased in the presence of neurons for 2 weeks ($n = 10$ for both groups). Action potentials could not be elicited (inset in i). (**b**) (i–ii) The inward current response by AMPA was blocked with CNQX and AP5, and the L-glutamate response was partially reduced. (iii) L-Glutamate–induced inward current was reduced by glutamate transporter inhibitors DHK and SOS. (**c**) Kinetics of cellular uptake of L-glutamate (starting at 50 μM) was measured in the absence or presence of PDC and Na^+ and normalized to μg of protein ($n = 3$ for each group). (**d**) Immature astrocytes propagate calcium waves to adjacent cells upon mechanical stimulation. Calcium wave propagation was measured for anterior and posterior immature astrocytes (20 s; retinoic acid = 59.2 μm ± 3.2, FGF8 = 76.0 μm ± 3.1, $P = 0.0196$. 30 s; retinoic acid = 62.4 μm ± 3.8, FGF8 = 91.4 μm ± 7.8, $P = 0.0288$, $n = 3$ (arrowheads) for all groups), both of which were inhibited by 2-APB (20 s p values; retinoic acid = 0.0144, FGF8 = 0.0104. 30 s p values; retinoic acid = 0.0147, FGF8 = 0.0197). (**e**) Co-culturing of hESC-derived neurons and immature astrocytes for 3 weeks results in an increased presence of Synapsin 1+ puncta (Syn, $n = 3$, $P = 0.0119$). Scale bars, 50 μm. Error bars, s.e.m. *, $P < 0.05$.

both retinoic acid–specified ($n = 18$) and FGF8-specified astroglia ($n = 10$, expanded for 120 d from line H9 and treated with CNTF for 7 d) displayed a voltage-dependent initial rapid outward current that was inactivated within 100 ms and a lower sustained current, and never displayed action potentials in current clamp. This passive electrophysiological property resembles that observed in immature primary mouse astrocytes[34]. To determine whether neuronal signaling promotes astroglial maturation, 120-d red fluorescent–labeled astroglia were cultured either with or without hESC-derived neurons (day 28) for 2 weeks (**Fig. 3a**). Co-cultured astroglia displayed a change in morphology and a significantly decreased transient outward current ($n = 10$ with and without neurons), suggesting maturation of astroglial cells *in vitro*.

One critical function of astrocytes is signaling and buffering of neurotransmitters released during neuronal excitation. To determine whether hESC-derived immature astrocytes contain functional glutamate receptors, we applied the glutamate receptor agonist AMPA or L-glutamate (100 μM) in the absence or presence of CNQX and AP5 (20 μM). An inward current was activated upon addition of AMPA, which was completely blocked in the presence of CNQX and AP5 (retinoic acid–specified, $n = 5$; FGF8-specified, $n = 5$) (**Fig. 3b**). In contrast, the L-glutamate response was partially blocked. L-glutamate induced a large inward current in all cells tested (retinoic acid–specified, $n = 8$; FGF8-specified, $n = 8$). 100 μM of D,L-aspartate produced a similar inward current (not shown). When the GLT-1–specific inhibitor dihydrokainate (DHK, 100 μM) was applied to the same cells for 1 min before L-glutamate administration, the inward current was substantially smaller, suggesting that glutamate-induced inward currents depend on the function of glutamate transporters. Addition of the general glutamate transporter blocker L-serine-*O*-sulfate (SOS, 100 μM) further decreased the current (**Fig. 3b**). No significant differences in induced currents were observed between the two subtypes of immature astrocytes owing to the high variability of peak currents between cells. Furthermore, hESC-derived immature anterior astrocytes were competent to take up glutamate from media over time at a higher rate than that of HEK293 cells, but not in the presence of the glutamate transporter inhibitor PDC or in sodium-free media ($n = 3$) (**Fig. 3c**). Together, these results indicate that the hESC-differentiated immature astrocytes possessed functional glutamate receptors and transporters.

Propagation of calcium waves across astrocytes, activated by various stimuli, is important in glial and neuron-glial communication[35], and calcium wave dynamics are different in regionally distinct astrocytes[18,19]. Fluorescent intensity of Fluo-4 loaded hESC (line H9)-derived 6-month immature astrocytes was observed during mechanical stimulation of a small area <20 μm. In all cells tested, stimulation induced an intra- and intercellular calcium wave in the vicinity, which traveled outward to adjacent cells (**Fig. 3d** and **Supplementary Movie 1**). Wave propagation was found to be dependent upon extracellular ATP signaling, because it was reduced by the presence of apyrase, an ATP hydrolytic enzyme, but not of the gap junction blocker carbenoxolone (**Supplementary Fig. 4**). The distance traveled by the calcium waves was different between retinoic acid– and FGF8-specified astroglia (**Fig. 3d**). Application of the InsP3 receptor blocker 2-APB[36] reduced the calcium wave distance for both retinoic acid– and FGF8-astroglial groups (**Fig. 3d**). Astroglia generated without FGF8 treatment, which also display anterior characteristics (**Supplementary Fig. 2b**), propagated waves in similar

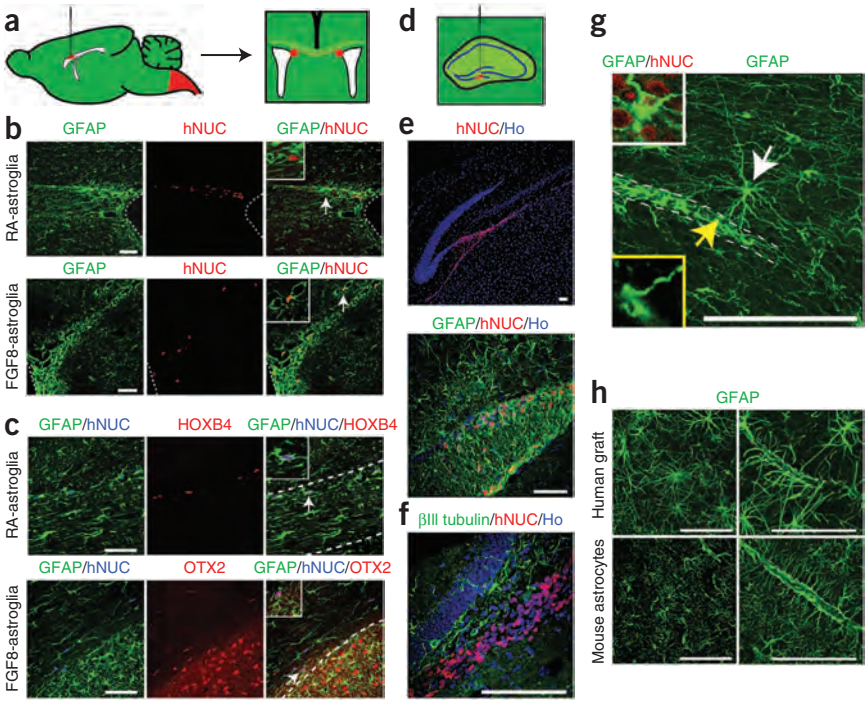

Figure 4 HPSC-derived astroglia retain their identity *in vivo*. (**a**) Illustration of intraventricular transplantation of hESC-derived astroglia and the resulting position of grafted cells. (**b**) One hundred days after transplantation, both retinoic acid–specified ($n = 3$) and FGF8-specified ($n = 4$) human cells (hNUC$^+$ = red) are present in ventricular areas (outlined with dashed lines), and express GFAP. Arrows indicate the human cells magnified in the insets. (**c**) Grafted, retinoic acid–specified human astrocytes (hNUC$^+$ = blue) in the corpus callosum (outlined with dashed lines) express HOXB4 (red, 65/65). In contrast, all of the FGF8-specified hNUC$^+$/GFAP$^+$ cells express OTX2 (red, 52/52). (**d**) Illustration of hippocampal transplantation. (**e**) Human astrocytes (red) survive and express GFAP but not βIII-tubulin (**f**) 6 weeks after transplantation to the adult hippocampus ($n = 4$ for each group). (**g**) Six months after transplantation of day 21 hESC-derived neural progenitors, human astrocytes (white arrow; hNUC$^+$/GFAP$^+$ shown in upper inset) extend processes onto endogenous blood vessels (outlined with dashes) with end feet (yellow arrow; shown in the lower inset on a single plane). (**h**) Mouse and human astrocytes exhibit distinct phenotypes, including process length and blood vessel association. Scale bars, 50 μm.

distances as that of the FGF8-specified astroglia (30 s; 106.5 ± 2.3 μm, $P = 0.1369$) and significantly different from that of retinoic acid–specified astroglia ($P < 0.001$) (data not shown). Thus, similar to astrocytes *in vivo*, hESC-derived immature astrocytes are competent for network communication.

Another function of astrocytes, especially immature astrocytes, is promotion of synaptogenesis[5,6,37]. To determine whether hPSC-derived immature astrocytes possess the same function, we cultured hESC-derived (day 21) neuronal progenitors alone, or in direct contact with immature astrocytes. The density of synapsin 1$^+$ puncta along the neurites was significantly ($P = 0.0119$) increased in neurons after 3 weeks of direct co-culture on hESC-derived (anterior) immature astrocytes compared to those without (**Fig. 3e**), suggesting the ability of hPSC-astrocytes to modulate synaptogenesis.

Regional and astroglial identity is retained *in vivo*

To determine whether hPSC-differentiated astroglia maintain their identity *in vivo*, we transplanted dissociated immature astrocytes, treated for 1 week with CNTF after 6 months of differentiation from line H9, into the lateral ventricles of neonatal mice (**Fig. 4a**). Thirty ($n = 2$ for retinoic acid group, $n = 2$ for FGF8 group) and 100 d ($n = 3$ for retinoic acid group, $n = 4$ for FGF8 group) after transplantation, grafted human cells, identified by human nuclear protein (hNUC), were observed as clusters adjacent to the lateral ventricles and as a stream of migrating cells in the corpus callosum. In every brain section examined, all of the transplanted hNUC$^+$ cells expressed a high level of GFAP (**Fig. 4b**,**c**). Cells that entered the corpus callosum were elongated in parallel with axons. Astroglial progenitor clusters (after 6 months without CNTF treatment, H9 line) transplanted directly into the adult mouse hippocampus also survived after engraftment (2 weeks; $n = 4$ for retinoic acid group and $n = 2$ for FGF8 group; 6 weeks; $n = 4$ for both groups) and continued to express GFAP (**Fig. 4d**,**e**), but not the neuronal marker βIII-tubulin$^+$, even in the neurogenic dentate gyrus (**Fig. 4f**). This result indicated that the hESC-derived astroglial progenitors or immature astrocytes retained their identity *in vivo*.

Immunostaining of the ventricle-transplanted cells for homeodomain transcription factors showed that all hNUC$^+$ cells in clusters and those migrating through the corpus callosum were positive for HOXB4 (day 30 = 70/70, day 100 = 65/65), but not for OTX2, and no hNUC-/GFAP$^+$ endogenous astrocytes in this region co-labeled with HOXB4 for the retinoic acid–specified astroglial group (**Fig. 4c**). In the brains transplanted with FGF8-specified immature astrocytes, all hNUC$^+$ cells were positive for OTX2 (day 100 = 52/52), but not HOXB4, and endogenous OTX2$^+$ astrocytes could be observed (**Fig. 4c**). Therefore, the regional specificity of astrocytes, which is acquired during early *in vitro* differentiation, is retained and not altered by the ectopic *in vivo* brain environment.

To determine whether *in vitro*–generated human astroglia can mature and integrate into the mouse brain, we examined whether they were in close apposition to blood vessels, a sign of contribution or signaling of astrocytes to the blood-brain barrier[38]. As blood-brain barrier formation requires coordinated development of blood vessels and astrocytes, we transplanted hESC-derived neural progenitors (day 21) to the ventricles of neonatal mouse brain and looked for direct connections of human GFAP$^+$ fibers to vessels. Few GFAP$^+$ cells were generated from grafted hESC-derived neuroepithelial cells within 3 months, as previously described[39]. However, 6 months after transplantation, a number of GFAP$^+$/hNUC$^+$ cells projected elongated fibers to blood vessels, with end feet directly contacting the vessels (**Fig. 4g**,**h** and **Supplementary Movie 2**). In contrast, endogenous mouse astrocytes are smaller, and the somas directly surround vessels. This distinction is similar to phenomena observed in adult human and rodent tissues[40]. These results indicate that the hPSC-derived astroglia can mature and participate in blood-brain barrier structure formation and that they exhibit some unique features of human astrocytes even in the mouse brain.

DISCUSSION

We have developed a chemically defined system for efficiently directing hPSC-derived neural progenitors to a nearly uniform population of astroglial progenitors and immature astrocytes through

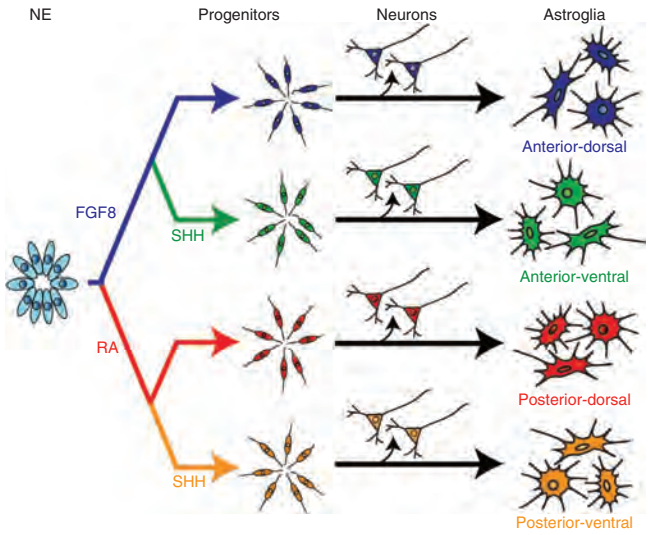

Figure 5 Hypothesis of astroglial subtype specification. The regional identity (anterior-posterior, dorsal-ventral) of astrocytes is determined when early neuroepithelial cells (NE, neural stem cells) are patterned to regional progenitors by morphogens such as retinoic acid and SHH. The regionalized progenitors first give rise to subclasses of neurons and then, during gliogenesis, generate regional-specific astrocytes with functionally distinct characteristics.

long-term expansion of dissociated progenitors in the presence of FGF2 and EGF. The *in vitro*–produced human immature astrocytes possess functional hallmarks of primary astrocytes, including responses to glutamate, propagation of calcium waves, promotion of synaptogenesis and participation in blood-brain barrier formation. Notably, we provide evidence that regionally and functionally diversified astroglial subtypes can be efficiently specified through patterning of early neuroepithelial cells with the same set of morphogens used for generating neuronal subtypes. Both astroglial identity and regional characteristics are maintained after long-term *in vitro* expansion and after transplantation into the mouse brain. Such human immature astrocytes, which can be generated in large quantities from an almost unlimited source of stem cells, should be useful in basic research, drug discovery and regenerative biology.

The regional and functional heterogeneity of astroglia has been well recognized[41]. However, it remains unclear whether this heterogeneity arises from intrinsic developmental programs or exclusively from adaptation to environmental cues. We have shown here that the regional identity of neuroepithelial cells, specified by a single morphogen, is maintained during subsequent differentiation. Comparisons of astroglial subtypes revealed differential onset of S100β and GFAP expression, cellular proliferation, gene expression and calcium wave propagation. Thus, the regional identity of astroglial cells is at least partially determined during neuroepithelial patterning, as has been previously postulated[22,42,43], and we propose that combinatorial morphogen patterning of neuroepithelial cells may lead to the generation of increasingly diversified astroglial subtypes (**Fig. 5**). This hypothesis suggests that regionalized neural progenitors migrate to target brain regions and then give rise to neurons before becoming astroglial cells, which may explain why we do not observe clear differential migration patterns of regionalized astroglia. Nevertheless, astroglial progenitors and immature astrocytes tend to target the white matter.

Functional properties of astroglia, particularly those of regional astroglia, are generally considered the outcome of responses to local brain environments[44]. Given the minimal presence of neurons and absence of immune cells in our culture system, our data suggest that at least some functions, described here, are intrinsic when astroglia are born. It should be pointed out that the astroglial cells in our culture system correspond to those at an early stage of the developing human brain. In the developed brain, astrocytes may well acquire additional mature functions, especially in response to local cues[45]. Furthermore, both the astroglial identity and regional characteristics are maintained after long-term *in vitro* expansion of their progenitors and after transplantation into the mouse brain environment. The intimate connections of hPSC-derived astrocytes with blood vessels suggest functional ability *in vivo*, though further work is needed to determine whether these cells can affect brain signaling or behavior.

Astrocytes in the human nervous system appear more complex than those in lower mammals[40]. Our present findings indicate that differentiation of human ESCs to a robust population of GFAP$^+$ astroglia (which takes at least 12 weeks) is substantially slower than that of mouse ESCs (which takes ~2 weeks), corresponding to astroglial development in the human brain. This prolonged development explains why hPSC-derived astroglial cells *in vitro* exhibit characteristics of immature rodent astrocytes *in vivo*, including the presence of voltage-gated currents[34] and induction of neuronal maturation[37]. Nevertheless, the immature astrocytes appear to mature over time when co-cultured with neurons or transplanted into the brain to participate in blood-brain barrier formation. Our ability to derive and expand an enriched population of astroglial progenitors, as well as to differentiate them to immature astrocytes, will facilitate studies of the role of human astrocytes in the normal and diseased brain and of transplantation therapies for neurological diseases such as amyotrophic lateral sclerosis, as suggested previously with mouse primary astrocytes[46]. In addition, astroglial cells derived from patient-specific iPSCs offer yet another approach for therapeutic discovery.

METHODS

Methods and any associated references are available in the online version of the paper at http://www.nature.com/naturebiotechnology/.

Note: Supplementary information is available on the Nature Biotechnology website.

ACKNOWLEDGMENTS

The authors thank A. Messing for critical reading of the manuscript. This study was supported by the ALS Association, National Institute of Neurological Disorders and Stroke (NS045926, NS057778, NS064578), National MS Society (NMSS TR-3761), NYSTEM (C024406), Bleser Family Foundation, Busta Family Foundation, Neuroscience Training Program (T32 GM007507) and partly by a core grant to the Waisman Center from the National Institute of Child Health and Human Development (P30 HD03352).

AUTHOR CONTRIBUTIONS

R.K. and S.-C.Z. designed the experiments and wrote the manuscript. R.K., J.P.W., Y.L. and Z.-J.Z. performed the experiments. R.K., J.P.W., Y.L., Z.-J.Z. and S.-C.Z. analyzed the data.

COMPETING FINANCIAL INTERESTS

The authors declare no competing financial interests.

Published online at http://www.nature.com/naturebiotechnology/.
Reprints and permissions information is available online at http://www.nature.com/reprints/index.html.

1. Barres, B.A. The mystery and magic of glia: a perspective on their roles in health and disease. *Neuron* **60**, 430–440 (2008).
2. Kettenmann, H. & Verkhratsky, A. Neuroglia: the 150 years after. *Trends Neurosci.* **31**, 653–659 (2008).
3. Zhang, S.C. Defining glial cells during CNS development. *Nat. Rev. Neurosci.* **2**, 840–843 (2001).

4. Rowitch, D.H. & Kriegstein, A.R. Developmental genetics of vertebrate glial-cell specification. *Nature* **468**, 214–222 (2010).
5. Ullian, E.M., Sapperstein, S.K., Christopherson, K.S. & Barres, B.A. Control of synapse number by glia. *Science* **291**, 657–661 (2001).
6. Johnson, M.A., Weick, J.P., Pearce, R.A. & Zhang, S.C. Functional neural development from human embryonic stem cells: accelerated synaptic activity via astrocyte coculture. *J. Neurosci.* **27**, 3069–3077 (2007).
7. Rothstein, J.D. *et al.* Knockout of glutamate transporters reveals a major role for astroglial transport in excitotoxicity and clearance of glutamate. *Neuron* **16**, 675–686 (1996).
8. Iadecola, C. & Nedergaard, M. Glial regulation of the cerebral microvasculature. *Nat. Neurosci.* **10**, 1369–1376 (2007).
9. Rouach, N., Koulakoff, A., Abudara, V., Willecke, K. & Giaume, C. Astroglial metabolic networks sustain hippocampal synaptic transmission. *Science* **322**, 1551–1555 (2008).
10. Oberheim, N.A. *et al.* Loss of astrocytic domain organization in the epileptic brain. *J. Neurosci.* **28**, 3264–3276 (2008).
11. Brenner, M. *et al.* Mutations in GFAP, encoding glial fibrillary acidic protein, are associated with Alexander disease. *Nat. Genet.* **27**, 117–120 (2001).
12. Seifert, G., Schilling, K. & Steinhauser, C. Astrocyte dysfunction in neurological disorders: a molecular perspective. *Nat. Rev. Neurosci.* **7**, 194–206 (2006).
13. Lobsiger, C.S. & Cleveland, D.W. Glial cells as intrinsic components of non-cell-autonomous neurodegenerative disease. *Nat. Neurosci.* **10**, 1355–1360 (2007).
14. Emsley, J.G. & Macklis, J.D. Astroglial heterogeneity closely reflects the neuronal-defined anatomy of the adult murine CNS. *Neuron Glia Biol.* **2**, 175–186 (2006).
15. Bachoo, R.M. *et al.* Molecular diversity of astrocytes with implications for neurological disorders. *Proc. Natl. Acad. Sci. USA* **101**, 8384–8389 (2004).
16. Yeh, T.H., Lee da, Y., Gianino, S.M. & Gutmann, D.H. Microarray analyses reveal regional astrocyte heterogeneity with implications for neurofibromatosis type 1 (NF1)-regulated glial proliferation. *Glia* **57**, 1239–1249 (2009).
17. Guatteo, E., Stanness, K.A. & Janigro, D. Hyperpolarization-activated ion currents in cultured rat cortical and spinal cord astrocytes. *Glia* **16**, 196–209 (1996).
18. Blomstrand, F., Aberg, N.D., Eriksson, P.S., Hansson, E. & Ronnback, L. Extent of intercellular calcium wave propagation is related to gap junction permeability and level of connexin-43 expression in astrocytes in primary cultures from four brain regions. *Neuroscience* **92**, 255–265 (1999).
19. Haas, B. *et al.* Activity-dependent ATP-waves in the mouse neocortex are independent from astrocytic calcium waves. *Cereb. Cortex* **16**, 237–246 (2006).
20. Muroyama, Y., Fujiwara, Y., Orkin, S.H. & Rowitch, D.H. Specification of astrocytes by bHLH protein SCL in a restricted region of the neural tube. *Nature* **438**, 360–363 (2005).
21. Sugimori, M. *et al.* Combinatorial actions of patterning and HLH transcription factors in the spatiotemporal control of neurogenesis and gliogenesis in the developing spinal cord. *Development* **134**, 1617–1629 (2007).
22. Hochstim, C., Deneen, B., Lukaszewicz, A., Zhou, Q. & Anderson, D.J. Identification of positionally distinct astrocyte subtypes whose identities are specified by a homeodomain code. *Cell* **133**, 510–522 (2008).
23. O'Leary, D.D., Chou, S.J. & Sahara, S. Area patterning of the mammalian cortex. *Neuron* **56**, 252–269 (2007).
24. Niederreither, K. & Dolle, P. Retinoic acid in development: towards an integrated view. *Nat. Rev. Genet.* **9**, 541–553 (2008).
25. Cahoy, J.D. *et al.* A transcriptome database for astrocytes, neurons, and oligodendrocytes: a new resource for understanding brain development and function. *J. Neurosci.* **28**, 264–278 (2008).
26. Nishiyama, A., Yang, Z. & Butt, A. Astrocytes and NG2-glia: what's in a name? *J. Anat.* **207**, 687–693 (2005).
27. Liu, Y. *et al.* CD44 expression identifies astrocyte-restricted precursor cells. *Dev. Biol.* **276**, 31–46 (2004).
28. Deneen, B. *et al.* The transcription factor NFIA controls the onset of gliogenesis in the developing spinal cord. *Neuron* **52**, 953–968 (2006).
29. Wilkinson, M., Hume, R., Strange, R. & Bell, J.E. Glial and neuronal differentiation in the human fetal brain 9–23 weeks of gestation. *Neuropathol. Appl. Neurobiol.* **16**, 193–204 (1990).
30. Pal, U., Chaudhury, S. & Sarkar, P.K. Tubulin and glial fibrillary acidic protein gene expression in developing fetal human brain at midgestation. *Neurochem. Res.* **24**, 637–641 (1999).
31. Hu, B.Y. *et al.* Neural differentiation of human induced pluripotent stem cells follows developmental principles but with variable potency. *Proc. Natl. Acad. Sci. USA* **107**, 4335–4340 (2010).
32. Pankratz, M.T. *et al.* Directed neural differentiation of human embryonic stem cells via an obligated primitive anterior stage. *Stem Cells* **25**, 1511–1520 (2007).
33. Li, X.J. *et al.* Coordination of sonic hedgehog and Wnt signaling determines ventral and dorsal telencephalic neuron types from human embryonic stem cells. *Development* **136**, 4055–4063 (2009).
34. Zhou, M., Schools, G.P. & Kimelberg, H.K. Development of GLAST$^+$ astrocytes and NG2$^+$ glia in rat hippocampus CA1: mature astrocytes are electrophysiologically passive. *J. Neurophysiol.* **95**, 134–143 (2006).
35. Scemes, E. & Giaume, C. Astrocyte calcium waves: what they are and what they do. *Glia* **54**, 716–725 (2006).
36. Doengi, M. *et al.* GABA uptake-dependent Ca^{2+} signaling in developing olfactory bulb astrocytes. *Proc. Natl. Acad. Sci. USA* **106**, 17570–17575 (2009).
37. Christopherson, K.S. *et al.* Thrombospondins are astrocyte-secreted proteins that promote CNS synaptogenesis. *Cell* **120**, 421–433 (2005).
38. Simard, M., Arcuino, G., Takano, T., Liu, Q.S. & Nedergaard, M. Signaling at the gliovascular interface. *J. Neurosci.* **23**, 9254–9262 (2003).
39. Guillaume, D.J., Johnson, M.A., Li, X.J. & Zhang, S.C. Human embryonic stem cell-derived neural precursors develop into neurons and integrate into the host brain. *J. Neurosci. Res.* **84**, 1165–1176 (2006).
40. Oberheim, N.A. *et al.* Uniquely hominid features of adult human astrocytes. *J. Neurosci.* **29**, 3276–3287 (2009).
41. Matyash, V. & Kettenmann, H. Heterogeneity in astrocyte morphology and physiology. *Brain Res. Rev.* **63**, 2–10 (2010).
42. Rowitch, D.H. Glial specification in the vertebrate neural tube. *Nat. Rev. Neurosci.* **5**, 409–419 (2004).
43. Kessaris, N., Pringle, N. & Richardson, W.D. Specification of CNS glia from neural stem cells in the embryonic neuroepithelium. *Phil. Trans. R. Soc. Lond. B* **363**, 71–85 (2008).
44. Hewett, J.A. Determinants of regional and local diversity within the astroglial lineage of the normal central nervous system. *J. Neurochem.* **110**, 1717–1736 (2009).
45. Silver, D.J. & Steindler, D.A. Common astrocytic programs during brain development, injury and cancer. *Trends Neurosci.* **32**, 303–311 (2009).
46. Lepore, A.C. *et al.* Focal transplantation-based astrocyte replacement is neuroprotective in a model of motor neuron disease. *Nat. Neurosci.* **11**, 1294–1301 (2008).

ONLINE METHODS

HPSC culture. HESCs (line H9, passages 20-30; H7, passages 35-40) and iPSCs ((IMR90)-4)[47] were cultured as previously described[32]. Briefly, cells were passaged weekly by dispase (1 mg/ml, Gibco) treatment and by plating on a layer of irradiated mouse embryonic fibroblasts. The hPSC medium consisted of DMEM/F12, 20% Knockout serum replacement, 0.1 mM β-mercaptoethanol, 1 mM L-glutamine, nonessential amino acids (Gibco) and 4 ng/ml FGF-2 (R&D Systems).

Differentiation of HPSCs. HPSCs were first differentiated to neuroepithelia for 10 d, as detailed elsewhere[48]. From days 10-21, cells were treated with either 0.5 μM of retinoic acid (Sigma), 50 ng/ml of FGF8 (Peprotech), or 500 ng/ml of sonic hedgehog (SHH, R&D Systems). Neural progenitors in a form of rosettes were blown off by a pipette at day 15 and expanded in a suspension culture containing EGF (Sigma) and FGF2 (R&D Systems, 10 ng/ml) starting from day 21. The neural progenitor spheres were disaggregated into small clusters with a Pasteur pipette to reduce cell contact, thus promoting gliogenesis instead of neurogenesis[49]. For astroglial differentiation, progenitor spheres were dissociated with accutase (Chemicon) to single cells, attached with a laminin substrate in the presence of CNTF (10 ng/ml, R&D System), LIF (10 ng/ml, Millipore), or FBS (FBS, 10%, Gibco). Cells were additionally passaged to coverslips for immunocytochemistry.

Immunochemistry and western blot. For immunocytochemistry, fixed cells were stained as previously described[32]. For quantification of each sample (n), 10 optic fields were chosen randomly under the fluorescent filter for nuclear staining throughout the coverslips in areas which contained a similar density of Hoechst$^+$ cells and the total cells were counted with Metamorph software. The fluorescent filters were shifted during imaging to count the cells labeled by different antibodies in the same field in the same manner. The quantitative data were repeated twice or more in different cultures or those from different cell lines. For western blotting, 30 μg of cell lysates were resolved with SDS-PAGE and transferred to nitrocellulose membranes. Detection was performed with horseradish peroxidase-conjugated secondary antibodies and the ECL system (Thermo Scientific). Primary antibodies are listed in **Supplementary Table 1**.

Proliferation assay. Cells were attached on coverslips for 48 h and treated with 0.2 μM 5-Bromo-2′-deoxyuridine (BrdU) for 10 h. Cells were fixed with methanol for 10 min, followed by incubation with 2 N HCL for 20 min. Cells were immunostained with the BrdU antibody as described above.

Quantitative reverse transcription polymerase chain reaction (qRT-PCR). cDNA was prepared using Superscript III First-Strand Synthesis System (Invitrogen). qRT-PCR was performed with Power SYBR Green PCR Master Mix (Applied Biosciences) on a StepOnePlus System with standard parameters and values were normalized to glyceraldehyde 3-phosphate dehydrogenase (GAPDH), $n = 3$ for each. The primer sets used are listed in **Supplementary Table 2**.

Primary culture. Primary astrocyte cultures were prepared from E13.5 timed pregnant CF-1 mice (Charles River). Brain regions were surgically dissected based on anatomical markers, dissociated with trypsin (Invitrogen), and cultured in DMEM + 10% FBS until experimentation. All experiments were performed with cells during passages 2–5.

Electrophysiology. Whole-cell patch clamp recordings were performed and analyzed as previously described[6]. During the procedure, cells were bathed in a modified Hank's Buffered Saline Solution (HBSS) that contained (in mM): 140 NaCl, 3 KCl, 2 $CaCl_2$, 1 $MgCl_2$, 15 HEPES and 23 glucose (pH 7.4, 300 mOsm). The following chemicals were applied through a gravity-fed drug barrel system: 4-aminopyridine (4-AP, 1mM), L-glutamate (100 μM), alpha-amino-3-hydroxyl-5-methyl-4-isoxazole-propionate (AMPA) (100 μM), (2R)-amino-5-phosphonopentanoate/6-cyano-7-nitroquinoxaline-2,3-dione (AP5/CNQX) (20 μM), D,L-aspartate (100 μM), dihydrokainic acid (DHK, 100 μM), and L-serine-*O*-sulfate (SOS, 100 μM), all obtained from Sigma. For co-culture experiments, immature astrocytes were infected with lentiviral particles to express transgenic mCherry protein driven by the cytomegalovirus promoter, and co-cultured without or with day 28 hESC-derived neurons in neural media as previously described[6].

Glutamate clearance assay. The method for measuring the decrease of glutamate over time[50] was modified. using the Glutamine/Glutamate Determination Kit (Sigma). Anterior astroglia were differentiated for 7 months, plated at a concentration of 20,000 cells per well in a 48-well plate, and cultured for an additional 7 d in the presence of CNTF. Before the assay, cultures were equilibrated in HBSS buffer for 10 min. 50 μM L-glutamate solutions were prepared with either HBSS ± L-*trans*-pyrrolidine-2,4-dicarboxylic acid (PDC, 1mM, Sigma) or Na^+ free HBSS (modified by replacing equimolar KCL with NaCl) and incubated with the cells. After various time periods, the glutamate concentration remaining in the media was measured at 340 nm following the enzymatic reaction. HEK293 cells, which do not significantly uptake glutamate compared to primary astrocytes, were used as controls. After subtraction of the blanks (0 glutamate added), the decrease in the media, or uptake of glutamate by cells, was reported as μM of glutamate per μg of protein after being normalized to the total protein in each well. The protein content was determined by a BCA protein assay (Pierce).

Calcium wave imaging. Astroglial cells were incubated at 25 °C with HBSS and 1 μl each of Fluor-4 (4 μM, Invitrogen) and Pluronic F-127 (0.01%, Invitrogen) for 30 min. Cells were washed with HBSS and imaged with an immersion objective on a confocal microscope (described below). Calcium wave induction was done by mechanical stimulation with a flame polished pulled glass pipette controlled manually with a micromanipulator (WPI). Five random fields were chosen under microscopy and averaged for each n. Fluorescent images were taken every 2 s with or without 2-aminoethoxydiphenyl borate (2-APB, Tocris, 100 μM), carbenoxolone (Sigma, 100 μM) or apyrase (Sigma, 50 units/ml). Calcium wave distances were quantified using Metamorph software. Post-fixation nuclear counting confirmed similar plating densities of astrocytes (retinoic acid = 121.3 ± 7.2, FGF8 = 125.7 ± 26.7 per 428 μm^2, $P = 0.88$).

Astrocyte-neuronal co-cultures for synaptogenesis studies. Human ESC-derived neural progenitors (day 21) were cultured in the neuronal differentiation media alone or directly on a layer of hESC-derived immature astrocytes (10,000 cells/cm^2) for 3 weeks, similar as previously described[6]. The cultures were then fixed with 4% paraformaldehyde and immunostained for βIII-tubulin and synapsin 1. Neurons with elongated neurites were chosen by visualization of βIII-tubulin under confocal microscopy. Fluorescent filters were then switched for Synapsin 1 imaging, and the synapsin 1+ puncta along the βIII-tubulin+ neurites were counted with ImageJ software. The results were expressed as the number of puncta per unit neurite length.

Transplantation. Transplantation studies were conducted following protocols approved by the Animal Care and Use Committees at the University of Wisconsin-Madison. Cells were prepared for transplantation in artificial cerebral spinal fluid (Harvard Apparatus) at a concentration of 50,000 cells/μl. For ventricle transplants, 2 μl of the cell suspension was injected 1 mm from the midline between the Bregma and Lambda and 1 mm deep into the anterior lateral ventricles of both hemispheres of severe combined immunodeficiency (SCID)-beige (Taconic) P1 mice. For transplantation into the adult SCID mouse hippocampus, 2 μl of cells were injected with the sterotaxic coordinates of −2.46 mm for anterior-posterior, ± 2 mm for lateral, and −2.25 mm for dorsal-ventral. At various time periods after transplantation, animals were anesthetized, perfused with 4% paraformaldehyde, and processed for immunohistochemistry with antibodies listed in **Supplementary Table 2**. Sections were imaged with a confocal microscope (Nikon, D-Eclipse C1), and EZ-C1 software (version 3.5).

Statistical analysis. Results were expressed as mean ± s.e.m. For quantification, each dataset (n) was generated from a separate passage of hPSCs. $n = 3$ unless noted differently. Fields were randomly selected and P values were calculated by unpaired t-test. *, $P \leq 0.05$.

47. Yu, J. *et al.* Induced pluripotent stem cell lines derived from human somatic cells. *Science* **318**, 1917–1920 (2007).
48. Hu, B.Y. & Zhang, S.C. Differentiation of spinal motor neurons from pluripotent human stem cells. *Nat. Protoc.* **4**, 1295–1304 (2009).
49. Caldwell, M.A. *et al.* Growth factors regulate the survival and fate of cells derived from human neurospheres. *Nat. Biotechnol.* **19**, 475–479 (2001).
50. Abe, K., Abe, Y. & Saito, H. Evaluation of L-glutamate clearance capacity of cultured rat cortical astrocytes. *Biol. Pharm. Bull.* **23**, 204–207 (2000).